Received: 22 July 2015 | Revised: 23 July 2017 | Accepted: 24 July 2017

DOI: 10.1002/nbm.3795

WILEY NMR IN BIOMEDICINE

RESEARCH ARTICLE

Value of whole breast magnetic resonance elastography added to MRI for lesion characterization

Corinne Balleyguier[1,2] | Aicha Ben Lakhdar[3] | Ariane Dunant[4] | Marie-Christine Mathieu[3] | Suzette Delaloge[5] | Ralph Sinkus[6,7,8]

[1] Radiology Department, Gustave Roussy, Villejuif, France

[2] Paris-Sud University, IR4M UMR 8081, Orsay, France

[3] Department of Medical Biology and Pathology, Gustave Roussy, Villejuif, France

[4] Department of Statistics, Gustave Roussy, Villejuif, France

[5] Department of Medical Oncology, Gustave Roussy, Villejuif, France

[6] Paris Diderot University, Sorbonne Paris Cité, France

[7] INSERM U773, Centre de Recherche Biomédicale Bichat-Beaujon, Paris, France

[8] BHF Centre of Excellence, Division of Imaging Sciences and Biomedical Engineering, King's College London, King's Health Partners, St. Thomas' Hospital, London, UK

Correspondence
Corinne Balleyguier, MD, PhD, Radiology Department, Gustave Roussy, 114 rue Edouard Vaillant, 94800 Villejuif, France.
Email: corinne.balleyguier@gustaveroussy.fr

Funding information
MEDICEN, Grant/Award Number: Darmus Ile-de-France

The purpose of this work was to assess the diagnostic value of magnetic resonance elastography (MRE) in addition to MRI to differentiate malignant from benign breast tumors, and the feasibility of performing MRE on the whole breast.

MRE quantified biomechanical properties within the entire breast (50 slices) using an 11 min acquisition protocol at an isotropic image acquisition resolution of 2 × 2 × 2 mm^3. Fifty patients were included. Finally, 43 patients (median age 52) with a suspect breast lesion detected by mammography and/or ultrasound were examined by MRI and MRE at 1.5 T. The viscoelastic parameters, i.e. elasticity (G_d), viscosity (G_l), the magnitude of the complex shear modulus $\sqrt{{G_d}^2 + {G_l}^2}$, and the phase angle $y = \frac{2}{\pi}\text{atan}\left(\frac{G_l}{G_d}\right)$, were measured via MRE and correlated with MRI Breast Imaging—Reporting and Data System (BI-RADS) score, histological type, and histological grade. Stroma component and angiogenesis were also correlated with viscoelastic properties.

In the 43 lesions, G_d decreased and y increased with the MRI BI-RADS score (p_{Gd} = 0.02, p_y = 0.002), whereas (G_l) and y were increased in malignant lesions (p_{Gl} = 0.045, p_y = 0.0004). The area under the curve increased from 0.84 for MRI BI-RADS alone to 0.92 with the MRI BI-RADS and y (AUC increase +0.08; 95% CI (−0.003; 0.16)). Lesion characterization using the y parameter increased the diagnostic accuracy. The phase angle y was found to have a significant role (p = 0.01) in predicting malignancy independently of the MRI BI-RADS. Interestingly, histological analysis showed no correlation between viscoelastic parameters and percentage and type of stroma, CD34 quantification of vessels, or histological grade.

The combination of MRE and MRI improves the diagnostic accuracy for breast lesions in the studied cohort. In particular, the phase angle y was found to have a significant role in predicting malignancy in addition to BI-RADS.

KEYWORDS

breast cancer, diagnosis, magnetic resonance elastography, MRI

1 | INTRODUCTION

Breast imaging is crucial in all steps of breast cancer management, from screening, diagnosis, and treatment choice to follow-up. Although mammography is the standard examination performed for screening and diagnosis,[1] it performs poorly in detecting lesions in women with dense breasts.[2] Here, ultrasound is better suited, and may be performed as a complement to standard X-ray mammography, but its specificity varies between 45 and 90%, depending on the aspect of the lesions, the type of equipment used, and the radiologist's experience.[3] MRI is the most sensitive imaging technique currently available, with a sensitivity estimated between 85 and 100%, and allows the detection of small lesions that

Abbreviations used: AUC, area under the receiver operating characteristic curve; BI-RADS, Breast Imaging—Reporting and Data System; IDC, invasive ductal carcinoma; ILC, invasive lobular carcinoma; MRE, magnetic resonance elastography; ROI, region of interest

are completely invisible on mammography or ultrasound; however, it is associated with a risk of false-positive diagnoses, estimated around 15 to 35%.[4] The consequences of such false-positive results are not negligible, as they lead to the biopsy of benign lesions, generating potential complications, unnecessary anxiety, and costs. It is estimated that up to 75% of biopsies following ultrasound are performed on benign lesions.[5] There is a need for new non-invasive imaging techniques to be developed and applied in clinical practice to improve the diagnostic accuracy and reduce false-positive diagnoses.[6]

Despite the frequent use of screening mammography, up to 43% of breast cancers are still discovered through manual palpation.[7] Clinical breast examination provides the first characterization of the lesions through the perceived differences in tissue firmness, as benign lesions tend to be soft, while malignant lesions tend to be stiff.[8] While the importance of manual palpation is undisputed in breast cancer detection and diagnosis, it lacks objectivity and precision, and its performance is limited in case of small or inaccessible lesions. Elastography is a relatively new non-invasive imaging technique that measures the tissue's mechanical properties, by assessing the propagation of mechanical waves through the tissue.[9] It can be considered as an objective and quantifiable way to measure tissue firmness that is perceived by palpation. Initial work in elasticity imaging was performed using ultrasound, and more recent investigations have included the approach using MRI.[10] Magnetic resonance elastography (MRE) is now a rapidly developing technique in the assessment of breast cancer as a complementary tool to MRI.[11,12]

Initial clinical results in breast MRE have shown promising results on MRE performance to improve MRI specificity.[13-16] However, most published studies to date have described MRE on breast phantoms, healthy volunteers, very small patient cohorts, or patients with relatively large lesions.[17-20] The diagnostic benefit of MRE has not yet been demonstrated in patients who would undergo MRI/MRE in an actual clinical setting, notably those presenting lesions that are difficult to characterize by mammography and ultrasound. In addition, the feasibility of MRE has remained an issue for routine use in clinical practice, due to the long duration required for partial imaging of the breast.

In this study, we aimed to evaluate first the diagnostic value of MRE in addition to MRI to differentiate malignant from benign tumors in patients with an indication for MRI, and second the feasibility of performing MRE on the whole breast. In addition, aiming for the identification of histological determinants of the variations in the tissue's mechanical properties, we also analyzed a potential link between viscoelastic properties and histological parameters.

2 | MATERIALS AND METHODS

2.1 | Patients

Women who were seen at our One Stop Breast Unit for a suspect lesion, for whom there was an indication for MRI, were asked to participate in the study. The median age was 52 (range 18–71 years). Participants were eligible for the study if they presented with a Breast Imaging—Reporting and Data System (BI-RADS) 3, 4, 5 breast lesion greater than 5 mm, detected by mammography and/or ultrasound. Exclusion criteria were contraindications for MRI, such as cardiac pacemakers, metallic implants, major claustrophobia, prior breast irradiation, pregnancy or breastfeeding, known allergy against the contrast agent (gadolinium chelate), and renal failure. Informed written consent was obtained from each participant before performing breast MRI. The participants' medical files were consulted to obtain their prior mammographic and ultrasound data. The study was approved by the ethical and scientific committees of our institution and a national consultative committee on data processing in biomedical research: CPP (Comité de Protection des Personnes) of Kremlin-Bicêtre Hospital where MRI was performed, CSET (Commission de Suivi des Essais Thérapeutiques) of Gustave Roussy, and CNIL (Commission Informatique et Liberté). MRI and MRE were performed prior to histological confirmation of the lesions.

2.2 | MRI and MRE of the breast

Initially, MRE data acquisition and image post-processing were optimized on a cohort of 10 volunteers. This first step allowed reduction of the MRE sequence length to an acceptable duration for clinical use (10 min, instead of 30 min). We developed an SE-EPI MRE sequence sensitive simultaneously with three different frequencies, 37.5 Hz, 75 Hz, and 112.5 Hz, combined. The resulting mechanical stimulus of three superimposed sinusoidal excitations allows for a time efficient diffusion of waves through the breast in a reduced time, enabling the potential integration of multi-frequency MRE into the standard clinical MRI breast protocol. However, elevated wave attenuation of the higher frequencies in some volunteers prevented us from utilizing this approach. Hence, the MRE sequence was tested on volunteers using a mono-chromatic mechanical excitation at 37.5 Hz.

A 1.5 T MR scanner (Achieva, Philips Healthcare, Best, The Netherlands) was used. An intravenous catheter was placed in a vein in the patient's arm or hand, and attached to a contrast media injector. The patient was then placed in the prone position with the two breasts placed in a dedicated coil with integrated mechanical transducers (Philips Research, Hamburg, Germany), and fixed by two adjustable transducer plates, which slightly compressed the breasts in the cranio-caudal direction. The plates transmitted mechanical waves at 37.5 Hz into the breast tissue, controlled via an external wave generator. Standard breast MR sequences were performed before the MRE sequences. Both MRI and MRE were performed without repositioning the patient.

MRI was performed as follows: sagittal T_1-weighted sequence without contrast agent, sagittal T_2-weighted sequence with fat suppression, sagittal (for the first five patients of the study) or axial dynamic T_1-weighted 3D gradient-echo with fat suppression before and after intravenous

contrast agent injection (0.1 mmol/kg) (Dotarem, Guerbet, Roissy, France). Dynamic contrast enhancement was quantified via a 3D T_1-weighted TFE sequence (T_E = 2.15 ms, T_R = 4.3 ms) providing six time points during a total acquisition time of ~6 min (in-plane resolution of 0.94 × 0.94 mm^2 and 2 mm slice thickness). Overall, total acquisition time regarding standard MR mammography protocols was approximately 15 min. The MRE sequence used a modified spin-echo sequence with EPI readout (T_E = 47 ms, T_R = 412 ms, 11 echoes), unilateral coverage of one breast with 50 slices and an isotropic pixel resolution of 2 × 2 × 2 mm^3. Four wave time offsets were sampled to capture the propagation of the mechanical wave. All three spatial directions were subsequently encoded. Using the above settings, MRE was successfully performed within a total acquisition time ranging between 10 and 12 min. The combination of an EPI factor of 11 and four time offsets enabled us to maintain a total scan time of about 10 min while significantly increasing the volume coverage.

2.3 | Image analyses

Evaluation of standard MRI images was done using a commercially available workstation (View Forum R6.3; Philips Healthcare) and post-processing tools dedicated to breast MRI (FuncTool, General Electric Healthcare, Chalfont St Giles, UK). MRE data were processed using a dedicated non-commercial software to obtain maps of viscoelastic properties (elasticity G_d, viscosity G_l, magnitude of complex shear modulus $|G^*| = \sqrt{{G_d}^2 + {G_l}^2}$, and phase angle $y = \frac{2}{\pi}\text{atan}\left(\frac{G_l}{G_d}\right)$).[15] Regions of interest (ROIs) were set manually by two operators in consensus (CB, RS), blinded to the histologic result, to enclose the corresponding lesion. ROIs were position on the post-contrast series with the best visibility of the lesion and then copied over—while maintaining geometry—to the corresponding maps of viscoelastic parameters to calculate corresponding average values of G_d, G_l, $|G^*|$, and y. The MRI BI-RADS score (1, normal; 2, typically benign; 3, probably benign (98% of benign lesion); 4, suspicious (10–95% of malignant lesion); 5, suggestive of a malignant lesion) was established from morphological and kinetic characteristics. We calculated the mean values within the ROIs for elasticity (G_d), viscosity (G_l), complex shear modulus ($|G^*|=\sqrt{{G_d}^2 + {G_l}^2}$), and phase angle $y = \frac{2}{\pi}\text{atan}\left(\frac{G_l}{G_d}\right)$.[15] All derived MRI and MRE parameters were compared with clinical data and with histopathology.

Radiologists performing the study had been informed prior to the MRE exam about the results of the previous imaging results for each patient.

2.4 | Histology

All BI-RADS 3 (with risk factors), 4, 5 breast lesions were cyto/histologically confirmed through fine needle aspiration (FNA) or biopsy. In addition to standard histological analysis (i.e. histological type, Elston-Ellis histological grade, hormone receptor status, human epidermal growth factor receptor 2 status), detailed histology regarding the stroma component and angiogenesis was performed in order to assess a potential link to biomechanical properties. For the analysis of stroma component and angiogenesis, histology was performed either on biopsied tissue samples for malignant lesions when treated with neoadjuvant chemotherapy, or on the surgical specimen when malignant lesions were operated without neoadjuvant therapy. The sections from formalin-fixed and paraffin-embedded tissues were analyzed by two experienced pathologists independently (MCM, ABL). Fibrosis evaluation was performed by two experienced pathologists in a consensual reading on hematoxylin–eosin safran staining on biopsy specimens in patients receiving neo-adjuvant chemotherapy, and on biopsy and surgical specimens when the patient was treated by surgery without any neoadjuvant chemotherapy. Safran stain allows colorization of collagen fibers. Fibrosis analysis was performed according to two main criteria: percentage of fibrosis according to the global surface of the specimen, and type of fibrosis, hyalinized or edematous, in a consensual visual assessment by both pathologists. A score of this analysis was defined in five grades (G1, 100% of peritumoral tissue edematous; G2, 75% edematous 25% hyalinized fibrous; G3, 50% edematous 50% hyalinized fibrous; G4, 25% edematous 75% hyalinized fibrous; G5, 100% fibrous). Angiogenesis was quantified in a × 200 field after staining with CD34 antibody, and classified into four grades (G1, 0–33; G2, 34–67; G3, 68–100; G4, >100).[21] Pathologists were blinded to the results of all imaging studies.

2.5 | Statistical analyses

Calculation of the necessary number of patients to include was based upon the McNemar exact test for paired series, with an acceptable power of 83% (software StatXact8, Cytel, Philips Research, Hamburg, Germany). A total of 50 patients is theoretically required to obtain a supposed increase of 40% of specificity with MRE in comparison with MRI, on the basis of a usual population of 40% of benign lesions in the population seen in our One Stop Breast Unit. Overall, 43 patients have been included in the current study. With 43 patients, keeping the same rate of benign lesions, the power goes down to 69%. With 43 patients and the observed 11 benign lesions, the power goes down to 25%. Since we are dealing with proportions, we do not provide effect size.

The association between viscoelastic parameters and different variables (MRI BI-RADS score, benign/malignant nature, histological grade, percentage and type of stroma, and CD34 quantification) was analyzed by linear regression, using the variables in classes to test heterogeneity. When classes were constructed from a quantitative variable, such as MRI BI-RADS score, trend tests were also provided, using the raw quantitative variable in the regression model.

The association between viscoelastic parameters and the histological grade, percentage and type of stroma, and CD34 quantification was analyzed by ANOVA for heterogeneity and by linear regression for trend analysis. A logistic model was used for the prediction of the benign/malignant nature of the lesion according to the MRI BI-RADS score alone or in conjunction with a viscoelastic parameter; results are presented and compared using receiver operating characteristic curves to determine the diagnostic value of adding the different viscoelastic parameters to MR-BI-RADS score. Areas under the curve (AUCs) are compared utilizing the DeLong test. Data were analyzed using SAS software, Version 9.1 (SAS Institute, Cary, NC, USA).

3 | RESULTS

3.1 | Patients and lesions

50 patients were initially recruited for the study. Seven patients were excluded due to technical failure. The seven technical failures were linked to MRE, with important movement artifacts impairing image quality and ability to obtain measurements. Overall, 43 patients were finally included in the study, all of whom had undergone mammography and ultrasound prior to undergoing MRI and MRE (Figure 1). Most patients presented with a single lesion (n = 38), whereas five patients had multiple lesions (two lesions in four patients and three lesions in one). For the purpose of this study, in the case of multiple lesions, only the largest lesion was taken into consideration. Following MRI, 3 lesions were classified MRI BI-RADS 3, 13 lesions BI-RADS 4 and 27 lesions BI-RADS 5.

Thirty-two lesions were malignant (74%) and 11 benign (26%). There were 22 invasive ductal carcinomas (IDCs), 8 invasive lobular carcinomas (ILCs), and 2 ductal carcinomas *in situ*. Among the IDCs and ILCs, eight malignant lesions were Grade 1 (27%), 15 were Grade 2 (50%), and 7 Grade 3 (23%). Most benign lesions were fibroadenomas (n = 9), one an inflammatory granuloma, and one fibrocystic disease.

3.2 | MRI

The median size of the lesions as assessed by MRI was 18 mm (range 4–75 mm). The morphological analysis of contrast-enhanced breast lesions showed that 34 lesions were masses (79%) and 9 lesions were non-mass-like enhancement. Figure 2A,B shows an example of an IDC, with a round mass that is moderately hyperintense on T_2-weighted sequence (A) and hypervascular with irregular margins (B).

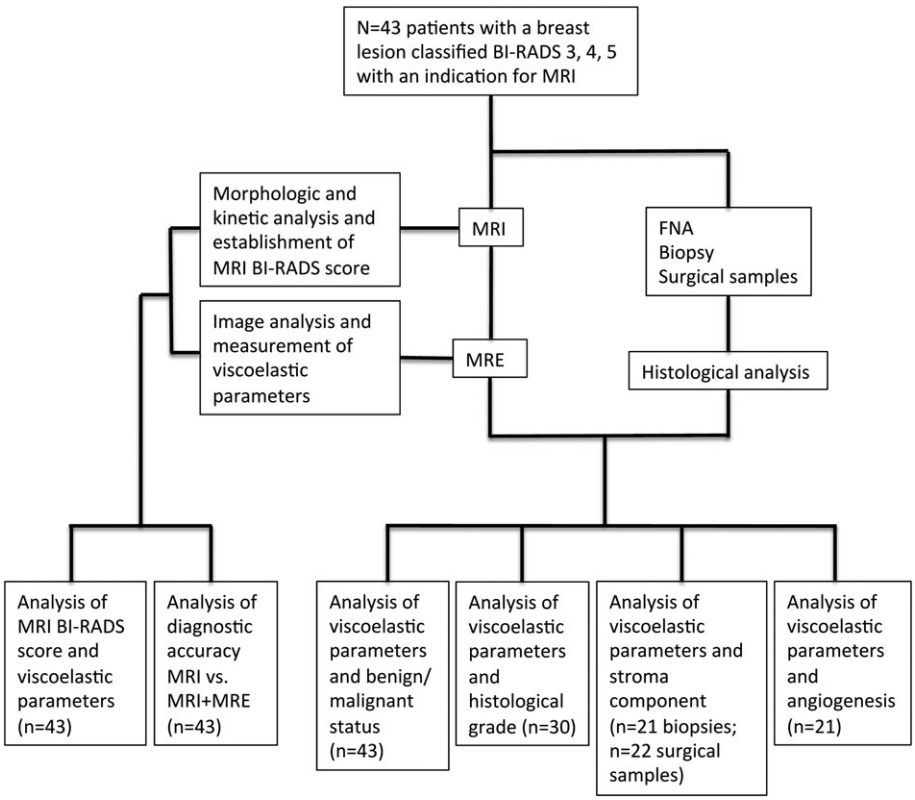

FIGURE 1 Study flow chart

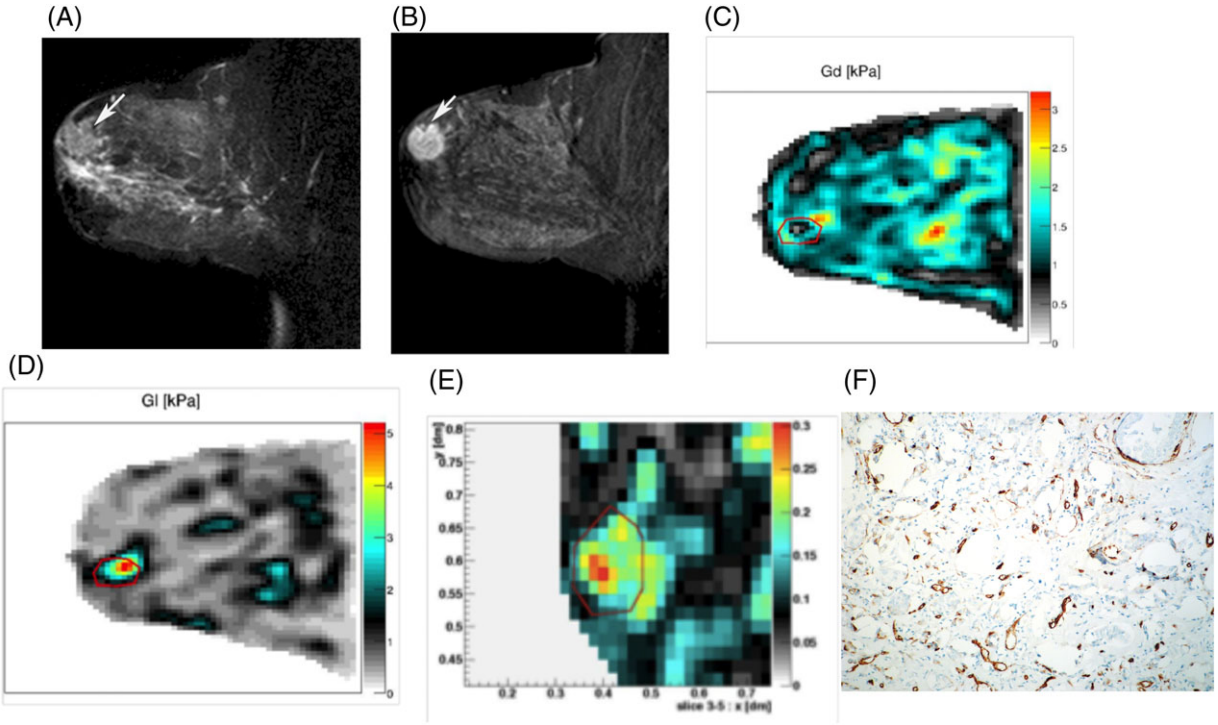

FIGURE 2 Images of a 25-year-old woman with an IDC grade 3. A,B, sagittal T2-w sequence, sagittal dynamic acquisition after injection: MRI morphologic analysis shows a round mass that is moderately hyperintense on T_2-weighted sequence (a) and hypervascular with irregular margins (B). C-E, MRE maps in an axial plan. MRE measurements show a low G_d (C), high G_l (D), and high y (E) ($|G^*|$ = 3.2 kPa, G_d = 1.34 kPa, G_l = 2.58 kPa, y = 0.59), corresponding to a lesion that is inelastic and highly viscous. F, CD 34 microvessel density evaluation, with a grade 4 evaluated on this analysis

3.3 | MRE

This specific MRE sequence enabled inspection of the biomechanical properties of the entire breast. The experimental setup, as well as the duration of MRI and MRE sequences, was well tolerated by all the patients.

In Figure 2, the target region reveals on the maps of the viscoelastic parameters low values of G_d (C), high values of G_l (D), and elevated values of y (E). Histologically, it was confirmed to be an IDC. Figure 3 shows an attenuating and irregular lesion that was occult on mammography (Figure 3 A), suspect on ultrasound (BI-RADS 5, Figure 3B), and hypervascularized on MRI (Figure 3C). The lesion showed high values of $|G^*|$ (Figure 3D) and elevated values of both y and G_l (Figure 3E). Histologically, it was confirmed to be an ILC.

Throughout the 43 lesions analyzed, correlation between elasticity (G_d) and MRI BI-RADS score shows that in the case of suspicious lesions the elasticity is reduced (n = 43, p = 0.02 for trend and p = 0.02 for heterogeneity) (Figure 4A), while the value of y increases with the MRI BI-RADS score concomitantly (n = 43, p = 0.002 for trend and p = 0.0004 for heterogeneity) (Figure 4B). Neither the viscosity (G_l) nor $|G^*|$ varied significantly with the MRI BI-RADS score. As for the relation between viscoelastic parameters and histology, viscosity (G_l) and y increased in malignant lesions (n = 43, p_{Gl} = 0.02, p < 0.0001) (Figure 4C,D), whereas G_d and $|G^*|$ did not vary with histology. The mean value of G_l was 0.75 kPa (range 0.28–2.58) for IDC, 0.57 kPa (range 0.38–1.04) for ILC, and 0.33 kPa (range 0.1–0.97) for benign lesions, and the mean value of y was 0.68 (range 0.47–0.9) for IDC, 0.67 (range 0.57–0.84) for ILC, and 0.35 (0.19–0.62) for benign lesions. Figure 4E shows the distinct distribution of G_d and y values for benign and malignant lesions (IDC and ILC), with an overlap between benign and malignant lesions, especially around G_d values lower than 0.5. No link could be established between histological grade and any of the viscoelastic parameters: G_d (heterogeneity p = 0.48, trend p = 0.94), G_l (heterogeneity p = 0.42, trend p = 0.94), y (heterogeneity p = 0.21, trend p = 0.99), and $|G^*|$ (heterogeneity p = 0.90, trend p = 0.93). Table 1 summarizes the mean results with standard deviation of all four MRE parameters ($|G^*|$, G_d, G_l, and y) for benign and malignant lesions.

In order to assess the value of MRE in addition to MRI, we analyzed the diagnostic accuracy by adding the y parameter to MRI BI-RADS score. Because of the small number of patients in each subtype of lesions, MRI BI-RADS 3 and 4 lesions were merged. Moreover, all BI-RADS 3 lesions were detected in high-risk women, and are usually biopsied. Indeed, in BRCA women some malignant lesions may appear with pseudo-benign round shape and smooth margins. The detection criteria were lesions with BI-RADS score 3 or 4 and y > 0.63, and lesions with BI-RADS score 5 and y > 0.22. Sensitivity, specificity, and positive and negative predictive values were respectively 0.79 (95% CI 61%–91%), 90% (95% CI 56%–100%), 96% (95% CI 81%–100%), and 56% (95% CI 30%–80%). AUCs based on 3/4 versus 5 categories were 0.84 for MRI only (95% CI 0.72–0.96) and 0.92 for MRI + y (95% CI 0.84–1.00) (Figure 5C). The difference in AUC is 0.08 (95%, CI −0.003; 0.16). Adding y to BI-RADS in the model for predicting the malignancy is interesting: the p value (log likelihood test) associated with y in

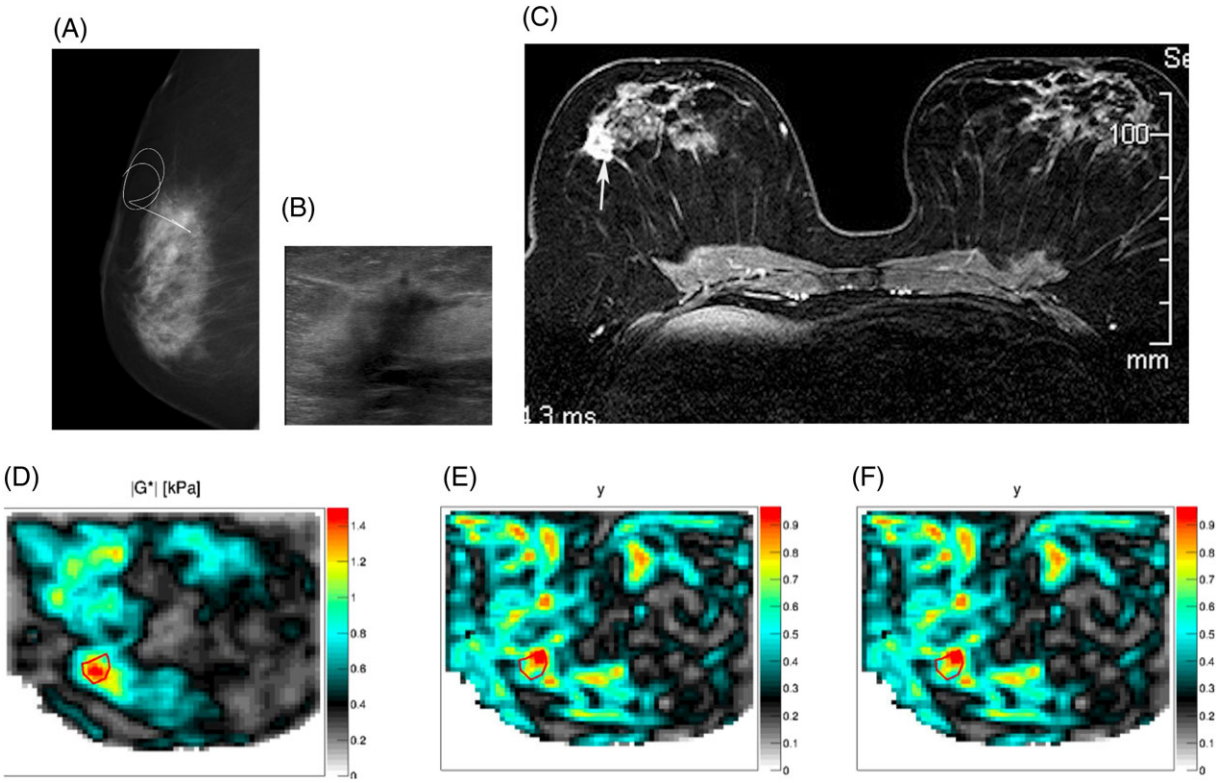

FIGURE 3 Images of a 58-year-old woman with an ILC grade 2. A,B, the lesion was almost occult on mammography (a) and presented an attenuating, irregular, suspect form on ultrasound (BI-RADS 5) (B). C, on MRI, after gadolinium-chelate injection, an irregular uptake is seen in the superior and outer quadrant of the right breast. D,E, MRE measurements showed a high G^* (D) and a high y (E) ($|G^*|$ = 1.25 kPa, G_d = 0.44 kPa, G_l = 1.04 kPa, y = 0.74). This high y value may be due to the histology of ILC, which is known to be more viscous than IDC

addition to BI-RADS is 0.01. Table 2 summarizes results for each of the four parameters. Besides y results, G_l and $|G^*|$ are also interesting for improving prediction.

3.4 | Histology

The median histological size of the lesions was 15 mm (range 5–70 mm). The stroma analysis was available in 43 lesions (21 biopsies and 22 surgical specimens). On the 21 biopsies, no relation was found between percentage of stroma component and any of the viscoelastic parameters: G_d (correlation = −0.17, p = 0.43), G_l (correlation = −0.11, p = 0.60), y (correlation = −0.29, p = 0.18), and $|G^*|$ (correlation = −0.14, p = 0.52). Equally, on 22 surgical samples, no relation was found between percentage of stroma component and any of the viscoelastic parameters: G_d (correlation = 0.09, p = 0.67), G_l (correlation = −0.04, p = 0.85), y (correlation = −0.04, p = 0.84), and $|G^*|$ (correlation = −0.00, p = 0.99). Angiogenesis was evaluable in 21 lesions (Figure 2F): no relation was observed between CD34 quantification and any of the viscoelastic parameters: G_d (heterogeneity p = 0.69, trend p = 0.82), G_l (heterogeneity p = 0.55, trend p = 0.81), y (heterogeneity p = 0.94, trend p = 0.71), and $|G^*|$ (heterogeneity p = 0.50, trend p = 0.98).

Analyses between lesion size and each of the four MRE parameters were the following: G_d, −0.31 (95% CI −0.63; +0.099), p = 0.13 NS; G_l, −0.07 (95% CI −0.45; 0.34), p = 0.75; y, 0.32 (95 CI −0.09; 0.63), p = 0.12; $|G^*|$, −0.17 (95% CI −0.54; 0.24), p = 0.41; none of the values is significantly different from zero, but this may be due to the lack of power of the study. Finally, we did not observe any potential link between tumor size and viscoelastic parameters.

4 | DISCUSSION

In this study, MRE increased (p = 0.06) the diagnostic accuracy of MRI, with an AUC value of 0.92 as compared with 0.84 for MRI alone. To our knowledge, this is the first study to show the value of MRE in a setting close to clinical practice, by examining only lesions left undetermined after mammography and ultrasound, in patients with an indication for MRI. The improvement of diagnostic accuracy using MRE is in partial agreement with some clinical studies. In a study involving 68 lesions (39 malignant and 29 benign), the combination of MRI and MRE resulted in an AUC value of 0.96, compared with 0.88 with MRI alone.[15] In another study with 57 lesions (37 malignant), MRE improved the diagnostic accuracy from an

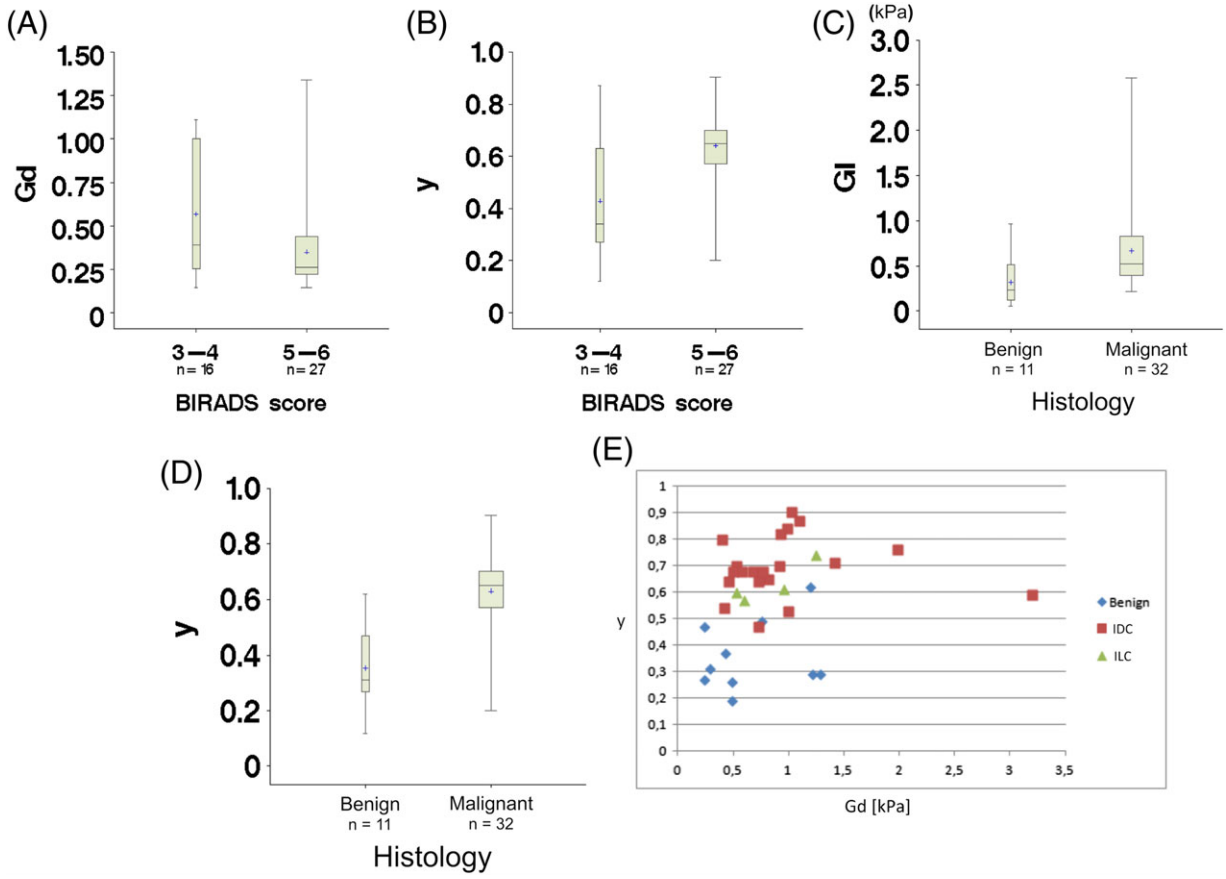

FIGURE 4 Correlation between viscoelastic parameters, MRI BI-RADS score, and histology. A, relation between G_d and MRI BI-RADS score: G_d decreases when BI-RADS score increases (p = 0.02). This is particularly clear for BI-RADS 3/4 and BI-RADS 5/6 lesions. B, relation between y and MRI BI-RADS score: y increases significantly when BI-RADS score also increases (p = 0.002). C, relation between G_l and histology: G_l increases in the case of malignant lesions (p = 0.02), especially for values higher than 0.6. D, relation between y and histology: y increases significantly in the case of malignant lesions, and in our study y was the best parameter to predict histological result (p < 0.0001). E, y and G_d values for various lesions with various pathological diagnoses: y increases in malignant lesions in comparison with benign lesions

TABLE 1 Summary of the mean results with standard deviation of all four MRE parameters ($|G^*|$, G_d, G_l, and y) for BI-RADS 3/4 and 5/6. Mean parameter (95% CI) in each group

Parameter	Bi-RADS 3/4	Bi-RADS 5/6	p (t test)
G_d	0.57 (0.37; 0.76)	0.35 (0.25; 0.44)	0.02
G_l	0.52 (0.29; 0.75)	0.63 (0.45; 0.81)	0.45
y	0.43 (0.31; 0.55)	0.64 (0.59; 0.70)	0.0004
G	0.87 (0.59; 1.15)	0.81 (0.59; 1.03)	0.74

AUC value of 0.93 with MRI alone to 0.96 with MRE.[14] Sinkus et al. observed a 20% increase in specificity (from 40 to 60%) at 100% sensitivity,[15] and Siegmann et al. also improved the specificity from 75% to 90% while maintaining a high sensitivity of 90%.[14]

In our study, due to the small numbers of BI-RADS 3 lesions, we decided to merge BI-RADS 3 and 4 lesions and compare MRI and MRI + y for BI-RADS 3/4 lesions with that for BI-RADS 5 lesions. Finally, for BI-RADS 3/4 lesions, any y value above the threshold of 0.63 would favor malignancy; as for BI-RADS 5 lesions, any y above the threshold of 0.22 would favor malignancy.

Our analysis of viscoelastic parameters and histology showed that both viscosity (G_l) and y were increased in malignant lesions. Siegmann et al. have observed significantly high values of both G_d and G_l in malignant lesions, compared with benign lesions, albeit with an overlap between malignant and benign lesions.[14] In the present study, y was found to be the best statistical parameter, and significantly correlated with the benign/malignant nature of the lesion, with nevertheless an overlap between benign and malignant lesions. The phase angle y was found to have a significant role (p = 0.01) in predicting malignancy, in addition to the MRI BI-RADS. We noted in our study that G_d decreased in malignant lesions as G_l increased, and this why the y parameter increases in the case of malignant lesions. As G_d is not significantly related to malignancy (p = 0.27), we can assume that the significant association with y is more induced by G_l. We preferred the y parameter, which is a combination of several viscoelastic properties of the lesions, and less sensitive to variations of one parameter, instead of G_l, even though G_l and G^* showed statistical links.

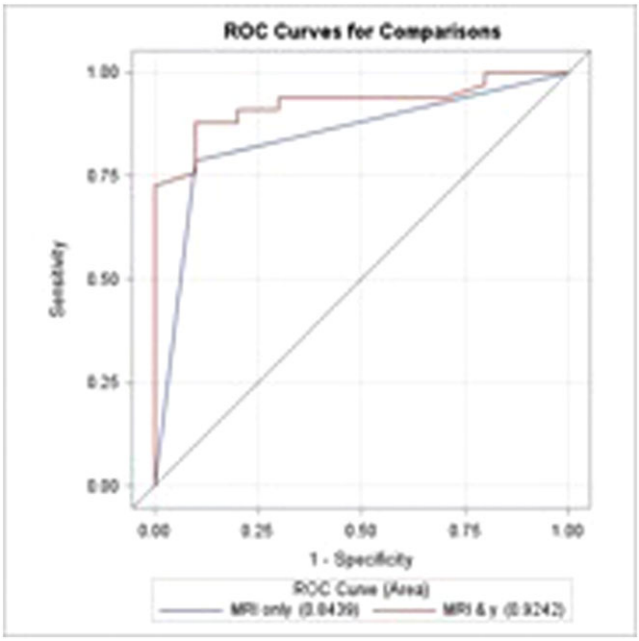

FIGURE 5 The performance of lesion categorization using MRI BI-RADS alone or with viscoelastic parameter y with respect to sensitivity and specificity. MRI only: AUC = 0.84 (95% CI 0.72; 0.96); MRI & y: AUC = 0.92 (95% CI 0.84; 1.00)

TABLE 2 MRE parameters added to MRI to predict malignancy

Parameter	Test of the interest of the MRE parameter in predicting malignancy in addition to MRI	AUC
y	$p = 0.01$	0.92 (0.84–1.00)
G_d	$p = 0.27$	0.90 (0.80–0.99)
G_l	$p = 0.005$	0.95 (0.89–1.00)
G	$p = 0.01$	0.94 (0.88–1.00)

We have shown that adding the *y* parameter, an objective and quantifiable element, to the MRI BI-RADS score can improve the classification and characterization of the lesions, thereby increasing the diagnostic accuracy. Importantly, the lesions we analyzed in the present study were smaller ($n = 43$, median size of 18 mm as assessed by MRI, range 4–75 mm) than those in previous studies, and many of them were complex lesions left undetermined after mammography and ultrasound. For comparison, Sinkus et al. analyzed 68 lesions, of which 39 were malignant lesions with a mean size of 28.5 mm,[15] and Siegmann et al. had 57 lesions with a mean size of 27.6 mm,[14] all lesions of much larger size. These changes in lesion population may have contributed to the different results shown in our study, in comparison with that of Sinkus et al.,[15] with a tendency to increase viscosity in malignant lesions. Nevertheless, the quantitative tumor parameters depend on several factors, such as tumor type, grade, tumor size, etc, and these results may be not reproducible in distinct studies, and should be interpreted carefully. The strength of our study lies in its proximity to the clinical setting in which MRI and MRE were performed. Biomechanics as quantified by MRE is most likely to be beneficial for the characterization and diagnosis of small, complex lesions. Nevertheless, correlation between MRE and BI-RADS may be moderated due to the small number of BI-RADS 3 lesions in our study.

Our results led us to test the hypothesis that changes in viscosity may also be linked to tumor grade. In histological analysis, however, we found no relation between G_d, G_l, *y*, or $|G^*|$ and CD34 quantification of vessels or histological grade. In addition, histological analysis did not show any relation between G_d, G_l, *y*, or $|G^*|$ and percentage of stroma component, although previous studies on MRE in hepatic fibrosis have shown the correlation between the increase in fibrosis and increase in elasticity.[22] Given the degree of heterogeneity in tumors even for the same type of lesion, it is possible that our sample size was too small to yield any significant histological correlation. Furthermore, elevated interstitial fluid pressure (IFP)—characteristic of malignant tumors—might represent a confounding factor, obstructing the expected relationship between angiogenic state and biomechanical properties. A larger study including a greater number of lesions in each subtype would be needed to analyze potential relationships between viscoelastic parameters and stroma characteristics or angiogenesis. Nonetheless, our results suggest that the phase angle *y* has a significant role in predicting malignancy, in addition to the MRI BI-RADS, and may be a potential functional marker to be considered in addition to the standard morphological and kinetic characteristics.

We optimized the MRE sequence in terms of spatial coverage and scan time when compared with previous studies.[13,14] As a result, we were able to acquire MRE data of the entire breast (50 slices of 2 mm thickness, 2 × 2 mm^2 in-plane resolution) within 10–12 min. This represents a considerable improvement over previous clinical studies that required 25 min or more for less than 10 slices,[13,16] as well as more recent studies

that required 10–12 min for seven slices.[14,15] Fifty slices allowed the coverage of up to 10 cm of the breast, which corresponded to the size of the entire breast in most cases. This optimized sequence makes MRE a highly feasible technique in daily clinical practice.

Our study has a few limitations. First, with 43 patients, our sample size is greater than that in some of the previous clinical studies, but still represents a relatively small cohort. With only 43 patients included in our study and the observed 11 benign lesions, the power is reduced to 25%. We have included a wide variety of malignant lesions as well as benign lesions that represent the most frequent lesions generally found in patients. Nonetheless, the number of patients in each sub-category was too small, especially ILC, to fully characterize the viscoelastic properties of each lesion type. Moreover, we did not find any correlation between tumor size and the viscoelastic parameters. This may be due to the lack of power of the study. In another previous study,[15] malignant tumors, significantly larger in size than the benign lesions, were quantified as more liquid-like in MRE. Additional, MRE was only performed on one lesion and on one breast in that study. Current limitations in sequence design and acquisition time prevent data acquisition of the contralateral side. Additional studies would be needed to develop and optimize the technique.

In conclusion, we have shown for this patient cohort that adding viscoelastic parameters as quantified by MRE to classical MR mammography increases the MRE diagnostic accuracy in lesions left undetermined after mammography and ultrasound. Phase angle is significantly correlated with the malignity of the tumor, and may be a potential functional marker for lesion characterization. In addition, we have considerably shortened the MRE acquisition time to 10–12 min per patient, while at the same time enabling full breast coverage. This enables application of breast MRE in clinical practice. Studies with larger patient cohorts will be necessary to further validate these results and to optimize the technique to provide bilateral biomechanical quantification.

ACKNOWLEDGEMENTS

Grant support: Darmus Ile-de-France.

ORCID

Corinne Balleyguier http://orcid.org/0000-0002-0018-8731

REFERENCES

1. de Koning HJ. Mammographic screening: evidence from randomised controlled trials. *Ann Oncol*. 2003;14(8):1185-1189.
2. Skaane P, Engedal K, Skjennald A. Interobserver variation in the interpretation of breast imaging. Comparison of mammography, ultrasonography, and both combined in the interpretation of palpable noncalcified breast masses. *Acta Radiol*. 1997;38(4 Pt 1):497-502.
3. Skaane P. Ultrasonography as adjunct to mammography in the evaluation of breast tumors. *Acta Radiol Suppl*. 1999;420:1-47.
4. Kuhl C. The current status of breast MR imaging. Part I. Choice of technique, image interpretation, diagnostic accuracy, and transfer to clinical practice. *Radiology*. 2007;244(2):356-378.
5. Stavros AT, Thickman D, Rapp CL, Dennis MA, Parker SH, Sisney GA. Solid breast nodules: use of sonography to distinguish between benign and malignant lesions. *Radiology*. 1995;196(1):123-134.
6. Kilburn-Toppin F, Barter SJ. New horizons in breast imaging. *Clin Oncol*. 2013;25(2):93-100.
7. Mathis KL, Hoskin TL, Boughey JC, et al. Palpable presentation of breast cancer persists in the era of screening mammography. *J Am Coll Surg*. 2010;210(3):314-318.
8. Krouskop TA, Wheeler TM, Kallel F, Garra BS, Hall T. Elastic moduli of breast and prostate tissues under compression. *Ultrason Imaging*. 1998;20(4):260-274.
9. Muthupillai R, Ehman RL. Magnetic resonance elastography. *Nat Med*. 1996;2(5):601-603.
10. Manduca A, Oliphant TE, Dresner MA, et al. Magnetic resonance elastography: non-invasive mapping of tissue elasticity. *Med Image Anal*. 2001;5(4):237-254.
11. Glaser KJ, Manduca A, Ehman RL. Review of MR elastography applications and recent developments. *J Magn Reson Imaging*. 2012;36(4):757-774.
12. Mariappan YK, Glaser KJ, Ehman RL. Magnetic resonance elastography: a review. *Clin Anat*. 2010;23(5):497-511.
13. Lorenzen J, Sinkus R, Lorenzen M, et al. MR elastography of the breast: preliminary clinical results. *Rofo*. 2002;174(7):830-834.
14. Siegmann KC, Xydeas T, Sinkus R, Kraemer B, Vogel U, Claussen CD. Diagnostic value of MR elastography in addition to contrast-enhanced MR imaging of the breast—initial clinical results. *Eur Radiol*. 2010;20(2):318-325.
15. Sinkus R, Siegmann K, Xydeas T, Tanter M, Claussen C, Fink M. MR elastography of breast lesions: understanding the solid/liquid duality can improve the specificity of contrast-enhanced MR mammography. *Magn Reson Med*. 2007;58(6):1135-1144.
16. Xydeas T, Siegmann K, Sinkus R, Krainick-Strobel U, Miller S, Claussen CD. Magnetic resonance elastography of the breast: correlation of signal intensity data with viscoelastic properties. *Invest Radiol*. 2005;40(7):412-420.
17. McKnight AL, Kugel JL, Rossman PJ, Manduca A, Hartmann LC, Ehman RL. MR elastography of breast cancer: preliminary results. *Am J Roentgenol*. 2002;178(6):1411-1417.
18. Sinkus R, Lorenzen J, Schrader D, Lorenzen M, Dargatz M, Holz D. High-resolution tensor MR elastography for breast tumour detection. *Phys Med Biol*. 2000;45(6):1649-1664.
19. Sinkus R, Tanter M, Catheline S, et al. Imaging anisotropic and viscous properties of breast tissue by magnetic resonance-elastography. *Magn Reson Med*. 2005;53(2):372-387.

20. Sinkus R, Tanter M, Xydeas T, Catheline S, Bercoff J, Fink M. Viscoelastic shear properties of in vivo breast lesions measured by MR elastography. *Magn Reson Imaging*. 2005;23(2):159-165.

21. Weidner N. Current pathologic methods for measuring intratumoral microvessel density within breast carcinoma and other solid tumors. *Breast Cancer Res Treat*. 1995;36(2):169-180.

22. Huwart L, Peeters F, Sinkus R, et al. Liver fibrosis: non-invasive assessment with MR elastography. *NMR Biomed*. 2006;19(2):173-179.

How to cite this article: Balleyguier C, Lakhdar AB, Dunant A, Mathieu M-C, Delaloge S, Sinkus R. Value of whole breast magnetic resonance elastography added to MRI for lesion characterization. *NMR in Biomedicine*. 2018;31:e3795. https://doi.org/10.1002/nbm.3795